

# Synthesis and Characterization of Poly(ethylene succinate) and Its Copolyesters Containing Minor Amounts of Butylene Succinate

Chi-He Chen, Hsin-Ying Lu, Ming Chen, Jyun-Siang Peng, Chia-Jung Tsai, Chao-Sen Yang

*Institute of Materials Science and Engineering, National Sun Yat-sen University, Kaohsiung 80424, Taiwan, Republic of China*

Received 27 April 2008; accepted 22 June 2008

DOI 10.1002/app.29035

Published online 30 October 2008 in Wiley InterScience (www.interscience.wiley.com).

**ABSTRACT:** Poly(ethylene succinate) (PES) and its copolyesters that contain 7, 10, or 48 mol % butylene succinate (BS) were synthesized through a direct polycondensation reaction with titanium tetraisopropoxide as the catalyst. Measurements of intrinsic viscosity (1.08–1.27 dL/g) proved the success of the preparation of polyesters with high molecular weights. The compositions and the sequence distributions of the copolyesters were determined from  $^1\text{H}$  and  $^{13}\text{C}$  NMR spectra. The distributions of ethylene succinate and BS units were found to be random. Their thermal properties were elucidated using a differential scanning calorimeter (DSC) and a thermogravimetric analyzer. No significant difference exists among the ther-

mal stabilities of these polyesters. All of the copolymers exhibit a single glass transition temperature. Wide-angle X-ray diffractograms (WAXD) were obtained from polyesters that were crystallized isothermally. The DSC thermograms and WAXD patterns indicate that the incorporation of BS units into PES significantly inhibits the crystallization behavior of PES. The heat of fusion of ideal PES crystals is 163 J/g, as determined by the depression of the melting point of PES crystals in acetophenone. © 2008 Wiley Periodicals, Inc. *J Appl Polym Sci* 111: 1433–1439, 2009

**Key words:** polyesters; copolymerization; NMR; thermal properties; WAXS

## INTRODUCTION

Problems of environmental pollution and waste management associated with bio-resistant synthetic plastics have become increasingly serious in the last several decades. With the rise of concern about the global environment, much attention has recently been paid to fully biodegradable polymers. Among biodegradable polymers, aliphatic polyesters have attracted considerable attention; they include poly(L-lactic acid), poly( $\epsilon$ -caprolactone), poly(ethylene succinate) (PES), poly(butylene succinate) (PBS), poly(3-hydroxyvalerate), and poly(4-hydroxybutyrate). These are considered to be biodegradable because of their susceptibilities to enzymes and microorganisms.<sup>1</sup>

PES and PBS are two commercial polyesters with a relatively high melting temperature and favorable mechanical properties,<sup>2</sup> which are similar to those of such extensively used polymers as low-density polyethylene and polypropylene. PBS exhibits a lower

biodegradation rate than PES because of its higher crystallization rate and crystallinity. A few approaches have been used to maintain their physical properties and to increase biodegradability; they include physical blending, copolymerization, and the formation of a composite with organoclay. With respect to copolymers,<sup>3–9</sup> degradation rates can be increased by incorporating small amounts of different kinds of diacids or diols, and this is basically attributed to the reduced crystallinity. The crystalline structure<sup>10–13</sup> and the crystal growth kinetics<sup>14,15</sup> of PES have been studied. Qiu et al.<sup>16,17</sup> have elucidated the isothermal and nonisothermal crystallization behavior of PES. The dependence of the crystallization rate and the primary nucleation rate of PES on molecular weight has also been investigated.<sup>18,19</sup> The crystalline structure,<sup>20–23</sup> crystallization, and melting behavior<sup>15,24–26</sup> of PBS have been examined. A series of PES and PBS copolymers have been synthesized and studied,<sup>6,27,28</sup> and a PBS-co-14%PES copolyester has been extensively reported.<sup>29,30</sup>

The degree of crystallinity, spherulite size, and lamellar structure of aliphatic polyesters affect the biodegradation rates, because biodegradation initially takes place in the amorphous region.<sup>31,32</sup> Therefore, estimating the degree of crystallinity from the ratio between the enthalpy of fusion and the heat of fusion of ideal crystals ( $\Delta H_u^0$ ) is important.

Correspondence to: M. Chen (mingchen@mail.nsysu.edu.tw).

Contract grant sponsor: National Science Council of the Republic of China, Taiwan; contract grant number: NSC 96-2221-E-110-045.

**TABLE I**  
**Composition, Probabilities of Triads, Randomness Factor ( $\beta$ ), and the Average Number Sequence Lengths ( $L_n$ ) of Synthesized Copolyesters**

Sample code	Composition		Normalized peak areas of the carbonyl carbons (%)				Triad sequence probabilities (%)			Composition			
	Feed ratio EG/BD	<sup>1</sup> H NMR ES/BS	ESE	ESB-E	ESB-B	BSB	P(ESE)	P(ESB)	P(BSB)	<sup>13</sup> C NMR ES/BS	$\beta$	$L_{nES}$	$L_{nBS}$
PEBSA 93/7	95/5	91.6/8.4	85.3	7.3	7.4	0.0	85.3	14.7	0.0	92.7/7.3	1.08	12.6	1.0
PEBSA 90/10	90/10	88.7/11.3	79.8	10.1	10.2	0.0	79.8	20.2	0.0	89.9/10.1	1.11	8.9	1.0
PEBSA 52/48	50/50	52.6/47.4	26.8	25.5	25.6	22.1	26.8	51.1	22.1	52.4/47.6	1.02	2.1	1.9

Flory and coworkers<sup>33–35</sup> proposed a method for evaluating  $\Delta H_u^0$  from the melting point depression in the polymer-diluent system. Malik and Nandi<sup>36</sup> used this method to estimate the heat of fusion of poly(3-alkyl thiophene)s. Recently, Papageorgiou and Bikiaris<sup>15</sup> estimated the  $\Delta H_u^0$  of PES by dividing the enthalpy of fusion obtained from the differential scanning calorimetry (DSC) data by the crystallinity ( $X_c$ ) determined from wide-angle X-ray diffraction (WAXD) pattern, giving a value of 180 J/g.

In this study, PES, PBS, and PES-rich copolyesters were synthesized. They were characterized using <sup>1</sup>H and <sup>13</sup>C NMR, DSC, thermogravimetric analyzer (TGA), and WAXD. The  $\Delta H_u^0$  value of PES was estimated from the melting point depression in the PES-acetophenone system according to the Flory equation.<sup>37</sup> Furthermore, the rates of cold crystallization and recrystallization of PES and PES-rich copolymers from the amorphous glass state are compared, and the degrees of crystallinity are also calculated from the enthalpy of melting during heating utilizing the obtained value of  $\Delta H_u^0$ .

## EXPERIMENTAL

### Materials

Ethylene glycol (EG) (Showa, 99.5%), 1,4-butanediol (BD) (Acros, 99%), and succinic acid (SA) (Acros, 99%) were used without purification. Titanium tetraisopropoxide (TTP) (Acros, 98+%) was used as received. Other solvents for the analysis were also used without purification.

### Synthesis

PES, PBS, and PES-rich copolyesters were synthesized by a two-step esterification reaction in the melt. The reactor was a 1 L stainless flask that was equipped with a magnetic agitator, an electric heater, a nitrogen inlet and outlet, a drain, a water cooling system, and a condenser. The reaction mixture was charged into the reactor with a diols : diacid molar ratio of 1 : 1. TTP was used as a cata-

lyst with a concentration of 0.1 mol % based on the amount of diacid used. The first two columns of Table I present the sample codes of copolyesters and the feed ratios of the diols. As an example, the synthesis of a copolyester with equal amounts of diols (PEBSA 52/48) is described as follows.

The reaction mixture of EG (31 g; 0.5 mol), BD (45 g; 0.5 mol), SA (118 g; 1 mol), and TTP catalyst (0.283 g; 1.0 mmol) was charged into the polycondensation reactor. The mixture was purged with nitrogen and heated with an electrical heater around the reactor. The temperature of the reactor was raised to 150°C to melt the acid component completely. Then the temperature was gradually raised to 190°C at 10°C/h. The water byproduct formed during the first stage was collected via a condenser. The condenser was kept at 100°C by an electrical heater for the separation of water from the monomers. The volume of water collected was 80 mol % of the theoretically calculated value. In the second stage of the reaction, the pressure was slowly reduced to below 1 Torr, and the temperature was raised to 220°C after 3 h of reaction. This condition was maintained for 20 h to facilitate further the reactions of polycondensation and transesterification. The synthesized polyester was dissolved in chloroform and precipitated into 10 times the amount of vigorously stirred ice-cooled methanol. The precipitate was filtered, washed with methanol, and dried under reduced pressure at room temperature. The other two copolyesters (PEBSA 93/7, PEBSA 90/10) and PES and PBS homopolymers were synthesized by the same procedures. Ivory white or pale brown polyesters were finally obtained.

These polyesters had intrinsic viscosity values,  $[\eta]$ , ranging from 1.08 to 1.27 dL/g measured in 60/40 w/w phenol/1,1,2,2-tetrachloroethane solution at 30°C (see the second column of Table II). PES had a  $[\eta]$  of 1.08 dL/g and a number average molecular weight of  $1.05 \times 10^5$  g/mol relative to poly(methyl methacrylate).<sup>38,39</sup> Therefore, the molecular weights of these synthesized aliphatic polyesters are sufficiently high for the subsequent studies.

**TABLE II**  
**Thermal Properties of Synthesized Polyesters**

Sample code	[ $\eta$ ] (dL/g)	$T_g$ ( $^{\circ}$ C)	$T_{cc}$ ( $^{\circ}$ C)	$T_m$ ( $^{\circ}$ C)
PES	1.08	-10.8	47.7	100.9
PEBSA 93/7	1.25	-11.7	53.3	94.5
PEBSA 90/10	1.14	-14.2	56.3	89.8
PEBSA 52/48	1.18	-29.1	-	37.8
PBS	1.27	-41.1	-15.5	113.1

### NMR analyses

NMR spectra of  $\text{CDCl}_3$  solutions were recorded with tetramethylsilane as the reference standard using a Varian UNITY INOVA-500 NMR at 295.5 K.  $^1\text{H}$  NMR spectra were analyzed to determine the compositions of the copolyesters.  $^{13}\text{C}$  NMR was utilized for the determination of both the composition and the ester sequence distribution in these copolyesters.

### Measurement of $\Delta H_u^0$

Experiments to measure  $\Delta H_u^0$  were conducted on a Perkin-Elmer Pyris 1 DSC, equipped with a refrigerating system (Pyris Intracooler 2P). The volume fractions of acetophenone solvent,  $\phi_1$ , were 0.311, 0.393, 0.466, 0.583, and 0.693, respectively. PES and solvent were sealed in a high-pressure pan, heated at a rate of  $20^{\circ}\text{C}/\text{min}$  from room temperature to  $70^{\circ}\text{C}$  above the melting peak temperature of each solution, and held for 5 min to erase any thermal history. The specimens were quenched at a maximum cooling rate to the chosen temperature, and then crystallized for 500–1000 min to ensure complete crystallization. After isothermal crystallization, the specimens were heated at  $10^{\circ}\text{C}/\text{min}$ . The melting temperatures were obtained from the deconvolution of the merged melting peaks.

The  $\Delta H_u^0$  value of PES was obtained from the depression of the melting point in PES-acetophenone mixture according to the following equation<sup>37</sup>:

$$\frac{1}{T_m^0} - \frac{1}{T_m} = \left( \frac{RV_2}{\Delta H_u^0 V_1} \right) [\phi_1 - \chi_1 \phi_1^2] \quad (1)$$

where  $T_m^0$  and  $T_m$  are the equilibrium melting temperatures of the pure polymer and polymer-diluent system, respectively;  $R$  represents the gas constant;  $V_1$  and  $V_2$  denote the molar volumes of the solvent and polymer, respectively; and  $\chi_1$  is the polymer-solvent interaction parameter.  $\chi_1$  can be expressed as  $BV_1/RT_m^0$ , where  $B$  is the interaction energy density. Equation (1) can be rearranged into a more convenient form.

$$\left( \frac{1}{T_m^0} - \frac{1}{T_m} \right) / \phi_1 = \frac{RV_2}{\Delta H_u^0 V_1} - \frac{BV_2}{\Delta H_u^0} \left( \frac{\phi_1}{T_m^0} \right) \quad (2)$$

Plotting  $(1/T_m^0 - 1/T_m)/\phi_1$  versus  $\phi_1/T_m^0$  yields a straight line. Then, the value of  $\Delta H_u^0$  can be calculated from the intercept of this plot.

### Measuring thermal properties

Compressed films with a thickness of about 0.2 mm were made and then dried in vacuum overnight at room temperature before use. A specimen with a diameter 6 mm and a weight about 4 mg was cut from a film and sealed in an aluminum pan. The thermal properties of the polyesters were analyzed using a Perkin-Elmer Pyris 1 DSC. The specimen was heated at a rate of  $20^{\circ}\text{C}/\text{min}$  to a chosen temperature, which was held for 5 min to remove the thermal history. Subsequently, the specimen was quenched with liquid nitrogen and then heated at a rate of  $10^{\circ}\text{C}/\text{min}$  to above its melting temperature ( $T_m$ ). The glass transition temperature ( $T_g$ ),  $T_m$ , and cold crystallization temperature ( $T_{cc}$ ) were detected during the heating process.

### Measurements of thermal stability

Thermal experiments were performed using a TA 2050 TGA. Nitrogen gas was used as the purge gas with a flow rate of 50 mL/min. A specimen of lighter than 10 mg was heated at a rate of  $10^{\circ}\text{C}/\text{min}$  from room temperature to  $800^{\circ}\text{C}$ . Weight loss curves and their derivatives were obtained to compare the relative thermal stabilities of the synthesized polyesters.

### WAXD measurements

Specimens with a thickness of about 0.5 mm following completely isothermal crystallization at a temperature of  $5$ – $20^{\circ}\text{C}$  below their respective  $T_m$  values were prepared using a heating stage (Linkam THMS-600). X-ray diffractograms were obtained on a Siemens D5000 diffractometer with Ni-filtered  $\text{Cu K}_\alpha$  radiation ( $\lambda = 0.1542$  nm, 40 kV, 30 mA) at a scanning rate of  $1^{\circ}/\text{min}$ . Measurements were made at room temperature.

## RESULTS AND DISCUSSION

### Copolyester composition and sequence distribution

Figure 1 presents the  $^1\text{H}$  NMR spectrum of PEBSA 52/48 copolymer and the peak assignments. The chemical shift of the protons of the succinic moiety ( $\text{H}_1$ ) is 2.60–2.70 ppm, whereas that of the protons

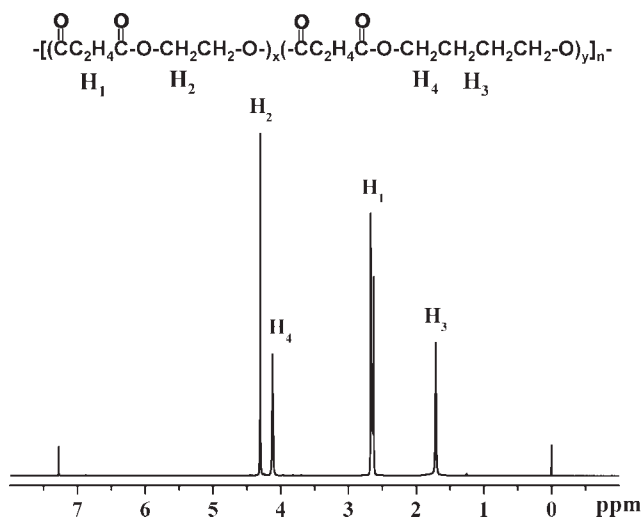


**Figure 1**  $^1\text{H}$  NMR spectrum of PEBSA 52/48 and peak assignments.

derived from EG monomer is  $\delta = 4.28\text{--}4.34$  ppm ( $\text{H}_2$ ). The two chemical shifts at 4.08–4.16 and 1.68–1.74 ppm are associated with the methylene protons  $\alpha$  ( $\text{H}_4$ ) and  $\beta$  ( $\text{H}_3$ ) bonded to the ester oxygen in the butylene succinate (BS) units. The composition of this copolyester is determined from the relative integration areas of these proton peaks. The mol % of BS moiety in PEBSA 52/48 is 47.4, as shown in the third column of Table I. Rows 1 and 2 of the same column present the compositions of the other two copolymers.

Figure 2 displays the  $^{13}\text{C}$  NMR spectrum of PEBSA 52/48. The chemical shifts of the ethylene carbons and the carbonyl carbons of the succinic moiety are at 28.70–29.00 ( $\text{C}_1$ ) and 171.94–172.30 ( $\text{C}_5$ ) ppm, respectively. The diol carbons derived from EG monomer are at 62.25–62.38 ppm ( $\text{C}_2$ ). For BS units, the chemical shifts of the carbons  $\alpha$  and  $\beta$  bonded to the ester oxygen are located at 64.08–64.20 ( $\text{C}_4$ ) and 25.11–25.22 ( $\text{C}_3$ ) ppm, respectively.

A magnified view of the  $^{13}\text{C}$  NMR spectrum of PEBSA 52/48 reveals that the carbonyl carbons ( $\text{C}_5$ ) are split into four peaks, as shown in the inserted spectrum of Figure 2. The peak  $\text{C}_{5a}$  is assigned to the carbonyl carbons with ethylene groups on both sides of the succinic ester, abbreviated as ESE. The assigned  $\text{C}_{5b}$ ,  $\text{C}_{5c}$ , and  $\text{C}_{5d}$  peaks represent the carbonyl carbons of the ESB-E side, ESB-B side, and BSB structures, respectively, as indicated in the inserted spectra in Figure 2 (where E represents the EG unit, S is the succinate unit, and B is the BS unit). The slight variation in chemical shifts of these four peaks is caused by the difference of the chemical environment, such that the integration areas can be utilized to characterize the chemical microstructures of these copolyesters.

The total areas of  $\text{C}_{5a}$ ,  $\text{C}_{5b}$ ,  $\text{C}_{5c}$ , and  $\text{C}_{5d}$  peaks are normalized to unity for each copolyester, and their percentage values of each peak area are listed in columns 4–7 of Table I under the subtitles of ESE, ESB-E side, ESB-B side, and BSB. Two peaks ( $\text{C}_{5b}$  and  $\text{C}_{5c}$ ) of equal intensity are observed from the unequivalent carbonyl carbons in the mixed diester sequence ESB. Three possible triad sequences, ESE, ESB, and BSB, of copolyesters are then calculated from the normalized areas, and tabulated in columns 8–10 of the same Table. In the case of PEBSA 52/48,  $P(\text{ESE})$ ,  $P(\text{ESB})$ , and  $P(\text{BSB})$  are 26.8, 51.1, and 22.1 mol %, respectively, as listed in the third row of Table I. The ES% and BS% of copolyesters are given by the following equations:

$$\text{ES}\% = P_{\text{ES}} = P(\text{ESE}) + P(\text{ESB})/2 \quad (3)$$

$$\text{BS}\% = P_{\text{BS}} = P(\text{BSB}) + P(\text{ESB})/2 \quad (4)$$

This copolyester is characterized by having 52.4 mol % ES units and 47.6 mol % BS units. Column 11 of Table I presents the ES% and BS% of other copolyesters.

The randomness,  $\beta$ , of the copolymer<sup>40,41</sup> is given by  $\beta = P(\text{ESB})/(2P_{\text{ES}} \times P_{\text{BS}})$ , where  $P_{\text{ES}}$  and  $P_{\text{BS}}$  are the molar fractions of ES and BS units calculated above. Copolyesters synthesized by polycondensation have generally been considered to have a random distribution. The results are due to the relatively equal reactivity of comonomers and the random transesterification during the polycondensation process. For total randomness of a copolymer,  $\beta$  is unity. The calculated  $\beta$  values of PEBSA 93/7, 90/10, and 52/48 are 1.08, 1.11, and 1.02, respectively,

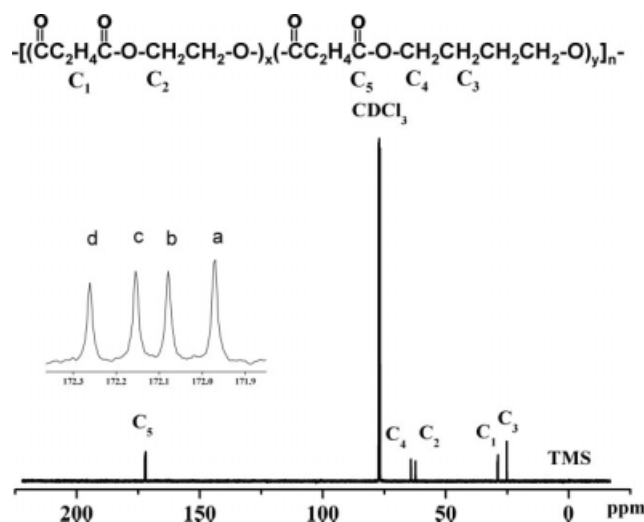


**Figure 2**  $^{13}\text{C}$  NMR spectrum of PEBSA 52/48 and peak assignments.

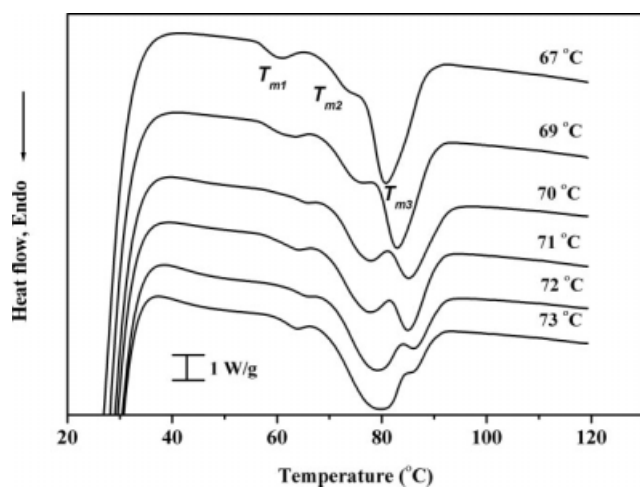


**Figure 3** DSC thermograms at a heating rate of 10°C/min for the PES-acetophenone ( $\phi_1 = 0.583$ ) mixture after complete crystallization at indicated temperatures.

as shown in column 12 of Table I. The distribution of ES and BS units in these copolyesters can be regarded as random. The reactivities of EG and BD with SA do not differ markedly. The average number sequence lengths<sup>40,41</sup> of ES and BS units are given by  $L_{nES} = 2P_{ES}/P(ESB)$  and  $L_{nBS} = 2P_{BS}/P(ESB)$ , respectively. In the case of PEBSA 52/48, they are 2.1 and 1.9, respectively. These values are listed in the last two columns of Table I. The values of  $L_{nBS}$  for PEBSA 93/7 and 90/10 are both 1.0.

### Heat of fusion ( $\Delta H_u^0$ ) of PES

Figure 3 shows the DSC heating thermograms obtained at a rate of 10°C/min from a PES-acetophenone ( $\phi_1 = 0.583$ ) mixture after completely isothermal crystallization ( $T_c$ ) at 67, 69, 70, 71, 72, and 73°C, respectively. Triple melting peaks are observed, and labeled as  $T_{m1}$ ,  $T_{m2}$ , and  $T_{m3}$  in order of increasing

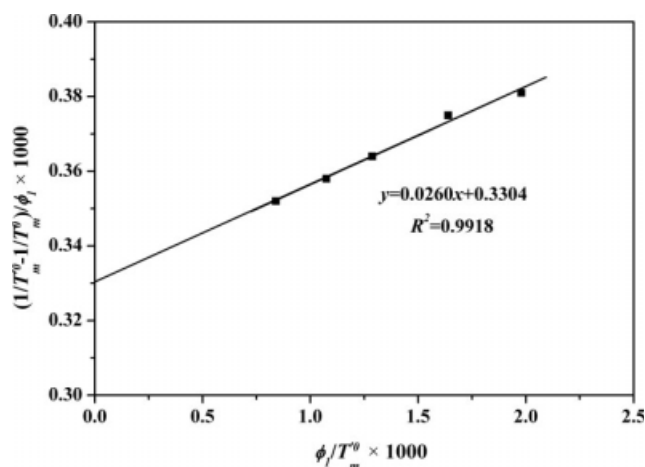


**Figure 4** Plot of  $(1/T_m^0 - 1/T_m^0)/\phi_1$  versus  $\phi_1/T_m^0$  for the PES-acetophenone mixtures.

temperature. The peak at  $T_{m2}$  shifts to higher temperature, and its intensity increases with  $T_c$ . The intensity of the peak at  $T_{m3}$  declines as  $T_c$  increases, and the ratio of the integrated areas of the peak at  $T_{m3}$  to that at  $T_{m2}$  also decreases. These results reveal that the peak at  $T_{m3}$  is associated with the melting of the recrystallized crystals, and the peak at  $T_{m2}$  is attributed to the fusion of the crystals that are grown during primary crystallization.<sup>42</sup> The peak temperatures ( $T_{m2}$ ) after deconvolution are plotted as a function of  $T_c$  to determine the equilibrium melting temperature of the PES-acetophenone mixture ( $T_m^0$ ) at a solvent volume fraction of 0.583. The Hoffman-Weeks approach yields a value of 82.7°C. The  $T_m^0$  values of the other volume fractions are obtained using the same method. They are 97.1°C for  $\phi_1 = 0.311$ , 92.9°C for  $\phi_1 = 0.393$ , 89.0°C for  $\phi_1 = 0.466$ , and 77.1°C for  $\phi_1 = 0.693$ . Clearly,  $T_m^0$  decreases as the volume fraction of the solvent increases. The values of each pair of  $T_m^0$  and  $\phi_1$  were used to estimate the heat of fusion of PES ( $\Delta H_u^0$ ) using eq. (2). The equilibrium melting temperature of PES ( $T_m^0$ ) obtained from previous investigation was 112.7°C.<sup>39</sup> Figure 4 plots the left-hand side of eq. (2) versus  $\phi_1/T_m^0$ . The intercept and the slope of a linear regression line yield  $\Delta H_u^0 = 163$  J/g and  $B = -5.72 \times 10^{-5}$  J/cm<sup>3</sup>. The numerical value of the heat of fusion of PES, determined in this study, is less than the value in the literature (180 J/g), estimated from WAXD crystallinity and DSC endothermic enthalpy.<sup>15</sup> In the following section, the value of 163 J/g is used in the calculation of the degree of crystallinity based on the heating traces of amorphous polyesters.

### Thermal properties

Figure 5 shows DSC heating curves of amorphous polyesters. PES has the highest  $T_g$  at -10.8°C.  $T_g$

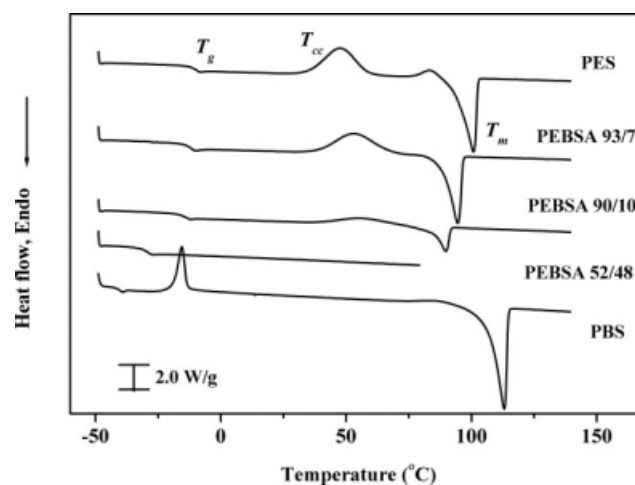


**Figure 5** DSC thermograms of amorphous polyesters at a heating rate of 10°C/min.

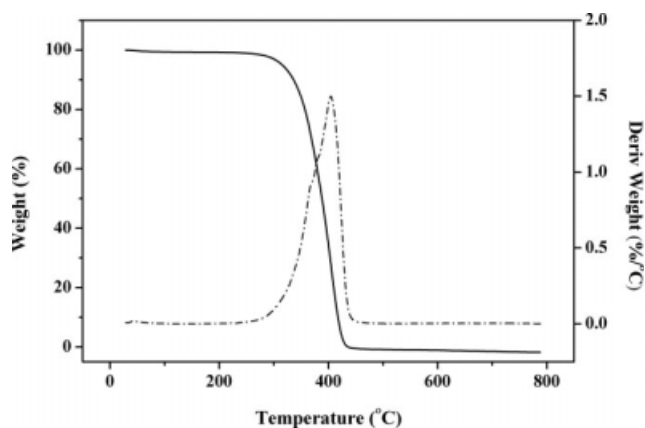


**Figure 6** Weight loss and its derivative for PEBSA 52/48 at a heating rate of 10°C/min under nitrogen.

gradually moves to a lower temperature as the moiety of the BS units increases. It ranges from  $-10.8$  to  $-41.1^{\circ}\text{C}$ , as listed in the third column of Table II. The copolyesters have intermediate  $T_g$  between those of the parent homopolyesters. Such  $T_g$  depression is attributed to the increase in the chain flexibility by the incorporation of BS units. Furthermore, all of the copolymers exhibit a single  $T_g$  value rather than two  $T_g$  values which would correspond to possible blocks of PES and PBS. Additionally, all of these copolyesters have  $\beta$  (randomness parameter) values of about 1.0, which are obtained from the  $^{13}\text{C}$  NMR analysis (Table I). These results demonstrate that the comonomer placement in these copolymers is essentially random.

A cold crystallization peak and a small recrystallization peak just before the melting peak are observed for PES and PBS homopolymers, as shown in Figure 5. The peak temperature of cold crystallization ( $T_{cc}$ ) occurs at  $-15.5^{\circ}\text{C}$  for PBS, and this peak is much sharper than that of PES ( $T_{cc}$  at  $47.7^{\circ}\text{C}$ ), indicating that the cold crystallization rate of PBS significantly exceeds that of PES. The thermogram of quenched PES reveals that the enthalpies of the cold crystallization ( $\Delta H_{cc}$ ), recrystallization ( $\Delta H_{rc}$ ), and melting ( $\Delta H_m$ ) are  $-40.3$ ,  $-4.9$ , and  $45.7$  J/g, respectively. A net enthalpy value of zero implies that amorphous PES was obtained after its thermal history was erased at  $170^{\circ}\text{C}$  for 5 min. The degrees of crystallinity caused by cold crystallization and recrystallization are 24.7 and 3.0%, respectively. The values of  $\Delta H_m$  of PEBSA 93/7 and PEBSA 90/10 are 44.9 and 18.5 J/g, respectively. The degrees of crystallinity calculated from  $\Delta H_m$  are 28.0% for PES, 27.5% for PEBSA 93/7, and 11.3% for PEBSA 90/10.

For PEBSA 93/7 and PEBSA 90/10,  $T_{cc}$  moves from  $53.3$  to  $56.3^{\circ}\text{C}$  (fourth column of Table II) and the corresponding peak becomes weaker and broader, as shown in Figure 5. No cold crystallization is detected in the curve of PEBSA 52/48.

Clearly, the incorporation of a few BS units into PES slows down the cold crystallization rate of amorphous specimens. Therefore, the intensity of the melting peak decreases, and the corresponding  $T_m$  falls from  $100.9$ , through  $94.5$  to  $89.8^{\circ}\text{C}$ , as listed in the last column of Table II. In the case of PEBSA 52/48,  $T_m$  was  $37.8^{\circ}\text{C}$  when the specimen kept at room temperature for more than 3 days.

### Thermal stability

Figure 6 plots the weight loss (solid curve) and the derivative of weight loss (dotted curve) versus temperature for PEBSA 52/48 copolyester in flowing nitrogen at a heating rate of  $10^{\circ}\text{C}/\text{min}$ . At temperatures below  $240^{\circ}\text{C}$ , the specimen appears to be stable; it exhibits noticeable weight loss only above  $241.1^{\circ}\text{C}$  (defined as  $T_{\text{start}}$  from the derivative curve of weight loss).  $T_{\text{loss}2\%}$  is defined as the temperature at a weight loss of 2% from the weight loss curve. It was  $285.4^{\circ}\text{C}$  for PEBSA 52/48. The rate of weight loss gradually increased to a maximum at  $404.5^{\circ}\text{C}$  (defined as  $T_{\text{max}}$  and identified from the derivative of the weight loss curve). Table III presents these three values for all of the polyesters used in this study, along with their average values. These polyesters exhibit no significant difference or no trend because the experiment depends on the size, shape, and crystallinity of the specimens.

### Wide angle X-ray diffraction

Figure 7 presents WAXD patterns of PES, PBS, and PES-rich copolyesters that were isothermally crystallized at  $5$ – $20^{\circ}\text{C}$  below their respective  $T_m$  values. The unit cell of the crystalline PES  $\alpha$  form is orthorhombic,<sup>12,13</sup> and the diffraction peaks from the (120) and (200) planes are observed at  $2\theta \approx 20.2^{\circ}$  and  $23.4^{\circ}$ , respectively. Both PEBSA 93/7 and 90/10 copolyesters have diffraction peaks of the PES  $\alpha$  form, but their intensity decreases as the moiety of the BS units increases. The unit cell of the crystalline PBS  $\alpha$  form is monoclinic,<sup>22,23</sup> and the diffraction peaks from the (020) and (110) planes are observed at  $2\theta \approx 19.6^{\circ}$  and  $22.7^{\circ}$ , respectively. The WAXD pattern of PEBSA 52/48 has the characteristic peaks of the PBS  $\alpha$  form, but with very low intensity.

**TABLE III**  
Thermal Stability of Synthesized Polyesters

Sample code	$T_{\text{start}}$ ( $^{\circ}\text{C}$ )	$T_{\text{loss}2\%}$ ( $^{\circ}\text{C}$ )	$T_{\text{max}}$ ( $^{\circ}\text{C}$ )
PES	247.1	291.9	379.5
PEBSA 93/7	248.1	283.9	387.4
PEBSA 90/10	242.1	277.9	398.2
PEBSA 52/48	241.1	285.4	404.5
PBS	246.1	298.5	400.3
Average	$244.9 \pm 3.1$	$287.5 \pm 7.9$	$394.0 \pm 10.3$

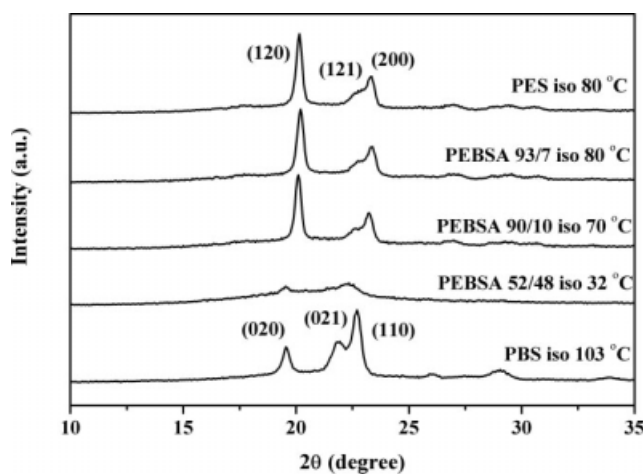


**Figure 7** WAXD patterns from polyesters crystallized at the temperatures indicated.

### CONCLUSIONS

Three PES-rich copolyesters were synthesized in a random sequence, as evidenced by a single  $T_g$  and a randomness value of near 1.0. Their intrinsic viscosities (1.08–1.27 dL/g) are sufficiently high to prove their relatively high molecular weight. The heat of fusion of ideal PES crystals,  $\Delta H_u^0 = 163$  J/g, is obtained from the depression in the melting point of the PES-acetophenone mixture. According to the compositions calculated from the  $^1\text{H}$  and  $^{13}\text{C}$  NMR spectra, the content of BS units incorporated into the copolyesters of PEBSA 93/7 and PEBSA 90/10 slightly exceeds that in the feed. Comparing the heating trace of amorphous PEBSA 93/7 with that of PES demonstrates that the peak temperature of the cold crystallization is delayed  $5.6^\circ\text{C}$  ( $53.3$  versus  $47.7^\circ\text{C}$ ); the difference between the degrees of crystallinity is only 0.5% (28.0% for PES minus 27.5% for PEBSA 93/7); however, the corresponding  $T_m$  value is lower at  $94.5^\circ\text{C}$  rather than  $100.9^\circ\text{C}$ . The heating thermograms of amorphous specimens and the WAXD patterns of crystallized specimens reveal that the incorporation of a few BS units into PES significantly inhibits the crystallization behavior of PES. The thermal stability of these polyesters does not vary significantly.

### References

- Mochizuki, M.; Hiram, M. *Polym Adv Technol* 1997, 8, 203.
- Doi, Y.; Steinbüchel, A. *Biopolymers vol. 4, Polyesters III—Applications and Commercial Products*; Wiley-VCH: Weinheim, Germany, 2002; Chapter 10.
- Montaudo, G.; Rizzarelli, P. *Polym Degrad Stab* 2000, 70, 305.
- Ahn, B. D.; Kim, S. H.; Kim, Y. H.; Yang, J. S. *J Appl Polym Sci* 2001, 82, 2808.
- Nikolic, M. S.; Djonlagic, J. *Polym Degrad Stab* 2001, 74, 263.
- Cao, A.; Okamura, T.; Nakayama, K.; Inoue, Y.; Masuda, T. *Polym Degrad Stab* 2002, 78, 107.
- Cao, A.; Okamura, T.; Ishiguro, C.; Nakayama, K.; Inoue, Y.; Masuda, T. *Polymer* 2002, 43, 671.
- Zhu, C. Y.; Zhang, Z. G.; Liu, Q. P.; Wang, Z. P.; Jin, J. *J Appl Polym Sci* 2003, 90, 982.
- Tserki, V.; Matzinos, P.; Pavlidou, E.; Vachliotis, D.; Panayiotou, C. *Polym Degrad Stab* 2006, 91, 367.
- Fuller, C. S.; Erickson, C. L. *J Am Chem Soc* 1937, 59, 344.
- Bunn, C. W. *Proc R Soc London* 1942, A180, 67.
- Ueda, A. S.; Chatani, Y.; Tadokoro, H. *Polym J* 1971, 2, 387.
- Ichikawa, Y.; Washiyama, J.; Moteki, Y.; Noguchi, K.; Okuyama, K. *Polym J* 1995, 27, 1264.
- Gan, Z. H.; Abe, H.; Doi, Y. *Biomacromolecules* 2000, 1, 704.
- Papageorgiou, G. Z.; Bikiaris, D. N. *Polymer* 2005, 46, 12081.
- Qiu, Z. B.; Ikehara, T.; Nishi, T. *Polymer* 2003, 44, 5429.
- Qiu, Z. B.; Fujinami, S.; Komura, M.; Nakajima, K.; Ikehara, T.; Nishi, T. *Polym J* 2004, 36, 642.
- Takayangi, M. *J Polym Sci* 1955, 19, 200.
- Umamoto, S.; Hayashi, R.; Kawano, R.; Kikutani, T.; Okui, N. *J Macromol Sci Phys* 2003, B42, 421.
- Chatani, Y.; Hasegawa, R.; Tadokoro, H. *Polym Prepr Jpn* 1971, 20, 420.
- Ichikawa, Y.; Suzski, J.; Washiyama, J.; Moeki, Y.; Noguchi, K.; Okuyama, K. *Polym J* 1995, 27, 1230.
- Ihn, K. J.; Yoo, E. S.; Im, S. S. *Macromolecules* 1995, 28, 2460.
- Ichikawa, Y.; Kondo, H.; Igarashi, Y.; Noguchi, K.; Okuyama, K.; Washiyama, J. *Polymer* 2000, 41, 4719.
- Yoo, E. S.; Im, S. S. *J Polym Sci Part B: Polym Phys* 1999, 37, 1357.
- Yasuniwa, M.; Satou, T. *J Polym Sci Part B: Polym Phys* 2002, 40, 2411.
- Yasuniwa, M.; Tsubakihara, S.; Satou, T.; Iura, K. *J Polym Sci Part B: Polym Phys* 2005, 43, 2039.
- Mochizuki, M.; Mukai, K.; Yamada, K.; Ichise, N.; Murase, S.; Iwaya, Y. *Macromolecules* 1997, 30, 7403.
- Yoo, Y. T.; Ko, M. S.; Han, S. B.; Kim, T. Y.; Im, S.; Kim, D. K. *Polym J* 1998, 30, 538.
- Gan, Z. H.; Abe, H.; Doi, Y. *Biomacromolecules* 2001, 2, 313.
- Gan, Z. H.; Abe, H.; Kurokawa, H.; Doi, Y. *Biomacromolecules* 2001, 2, 605.
- Kumagai, Y.; Kanesawa, Y.; Doi, Y. *Makromol Chem* 1992, 193, 53.
- Iwata, T.; Doi, Y. *Macromol Chem Phys* 1999, 200, 2429.
- Flory, P. J.; Mandelkern, L.; Hall, H. K. *J Am Chem Soc* 1951, 73, 2532.
- Mandelkern, L.; Garrett, R. R.; Flory, P. J. *J Am Chem Soc* 1952, 74, 3949.
- Evans, R. D.; Mighton, H. R.; Flory, P. J. *J Am Chem Soc* 1950, 72, 2018.
- Malik, S.; Nandi, A. K. *J Polym Sci Part B: Polym Phys* 2002, 40, 2073.
- Flory, P. J. *Principles of Polymer Chemistry*; Cornell University Press: Ithaca, NY, 1953; p 569.
- Tsai, C. J.; Chang, W. C.; Chen, C. H.; Lu, H. Y.; Chen, M. *Eur Polym J* 2008, 44, 2339.
- Lu, H. Y.; Peng, J. S.; Chen, M.; Chang, W. C.; Chen, C. H.; Tsai, C. J. *Eur Polym J* 2007, 43, 2630.
- Backson, S. C. E.; Kenwright, A. M.; Richards, R. W. *Polymer* 1995, 36, 1991.
- Ko, C. Y.; Chen, M.; Wang, H. C.; Tseng, I. M. *Polymer* 2005, 46, 8752.
- Chen, M.; Chang, W. C.; Lu, H. Y.; Chen, C. H.; Peng, J. S.; Tsai, C. J. *Polymer* 2007, 48, 5408.